POLITECNICO
MILANO 1863

De-tumbling and Nadir Pointing Simulation of 16 U Cubesat

Spacecraft Attitude Dynamics and Control (A.Y. 2020/21)

Nugraha Setya Ardi (952035-10714522)

nugrahasetya@mail.polimi.it

Contents

I. Introduction

In this report we present a simulation of 16 U cubesat orbiting low earth orbit using Simulink. The cubesat is modeled with 3 reaction wheels, gyro sensor, earth horizon sensor, star sensor, and sun sensor. SVD method is used to determine the attitude and state observer is employed as filtering method. A proportional feedback and DCM-based control law are used to perform detumbling and nadir pointing. Some disturbances which are simulated are magnetic torque, solar radiation pressure, and gravity gradient torque. The cubesat and reaction wheels are assumed to have diagonal matrix of mass inertia.

II. Modeling

In this section some aspects for modeling are explained.

a. Spacecraft Physical Model

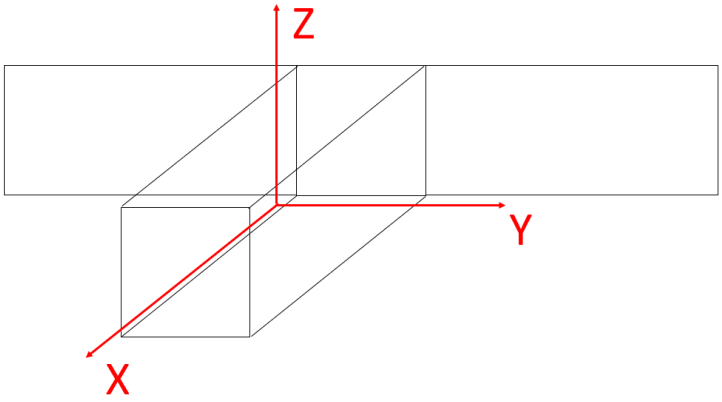

Figure 1. Spacecraft model and its body axis.

The model of the spacecraft and its body axis is depicted by figure 1. It has two solar panel mounted on its side. Its properties are given by

Table 1. Properties of spacecraft**.**

	Mass [kg]	Size [m]
Main body	12.0	0.4 × 0.2 × 0.2
Solar panels (single panel)	0.6	0.4 × 0.2

$$I_{sc} = \begin{bmatrix} 0.11 & 0 & 0 \\ 0 & 0.2 & 0 \\ 0 & 0 & 0.23 \end{bmatrix} kg.m^2$$

$$x_{cg} = [0.01 \quad 0 \quad 0]^{\top} m$$

b. Global Simulink Model

The scheme of Simulink model is given by the following figure.

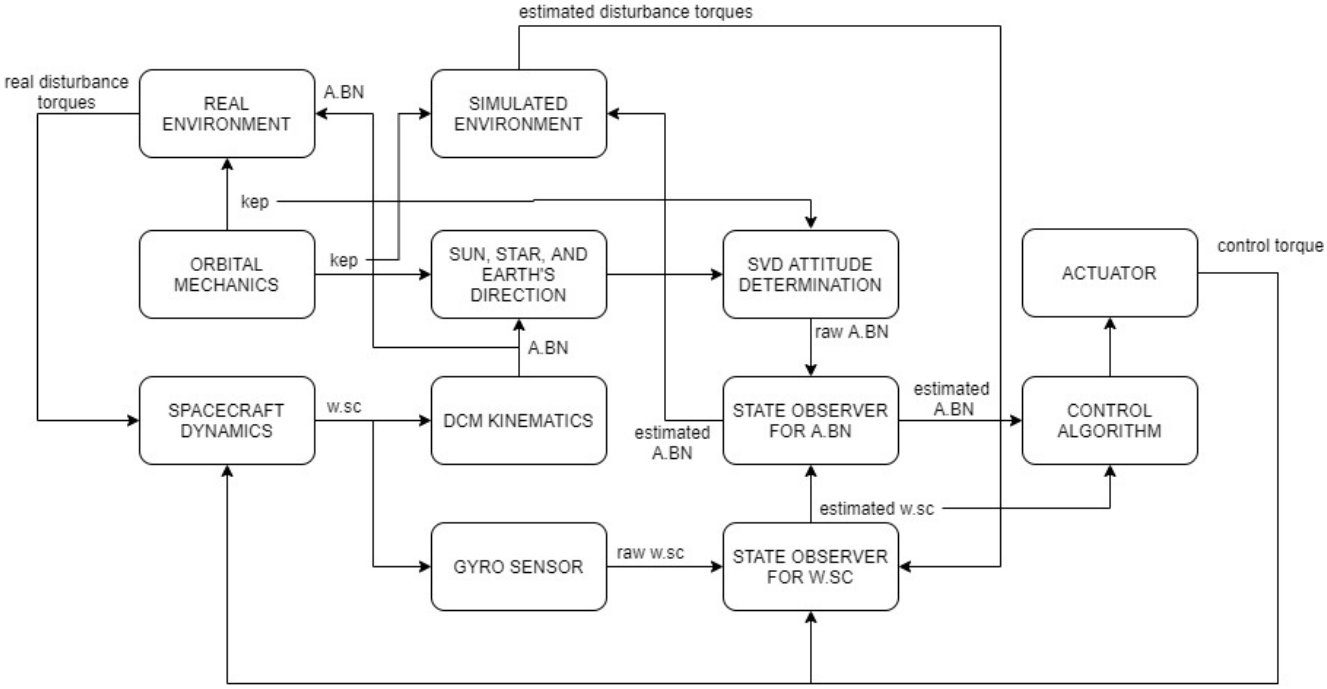

Figure 2. Scheme of Simulink model.

c. Spacecraft and Reaction Wheel's Dynamics

The dynamics of spacecraft and three axis reaction wheels are modeled as follows:
First, the total angular momentum of spacecraft and reaction wheels are given by

$$\vec{h}_{tot} = \boldsymbol{I}_{sc}\vec{\omega}_{sc} + \boldsymbol{I}_{rw}\vec{\omega}_{rw}$$

Then the external disturbance torque makes the angular momentum to change with respect to time

$$\dot{\vec{h}}_{tot} = \vec{T}_{ext}$$

$$\dot{\vec{h}}_{tot} = \boldsymbol{I}_{sc}\dot{\vec{\omega}}_{sc} + \vec{\omega}_{sc} \times (\boldsymbol{I}_{sc}\vec{\omega}_{sc}) + \boldsymbol{I}_{rw}\dot{\vec{\omega}}_{rw} + \vec{\omega}_{sc} \times (\boldsymbol{I}_{rw}\vec{\omega}_{rw}) = \vec{T}_{ext}$$

And finally, we can express $\dot{\vec{\omega}}_{sc}$ as

$$\dot{\vec{\omega}}_{sc} = \boldsymbol{I}_{sc}{}^{-1}(\vec{T}_{ext} - (\vec{\omega}_{sc} \times (\boldsymbol{I}_{sc}\vec{\omega}_{sc}) + \boldsymbol{I}_{rw}\dot{\vec{\omega}}_{rw} + \vec{\omega}_{sc} \times (\boldsymbol{I}_{rw}\vec{\omega}_{rw}))) \qquad (1)$$

In the equation above, $\vec{T}_{ext}$ is the sum of all external disturbance torques like gravity gradient torque, solar radiation pressure torque, and magnetic torque. The control inputs are through $\dot{\vec{\omega}}_{rw}$ and $\vec{\omega}_{rw}$. To compute these, we can define

$$\dot{\vec{\omega}}_{sc} = \boldsymbol{I}_{sc}{}^{-1}(\vec{T}_{ext} - (\vec{\omega}_{sc} \times (\boldsymbol{I}_{sc}\vec{\omega}_{sc}) + \vec{M}_c)$$

Where $\vec{M}_c$ is the required torque to control the spacecraft, and is given by

$$\vec{M}_c = -\boldsymbol{I}_{rw}\dot{\vec{\omega}}_{rw} - \vec{\omega}_{sc} \times (\boldsymbol{I}_{rw}\vec{\omega}_{rw}) \tag{2}$$

where

$$\dot{\vec{\omega}}_{rw} = \begin{bmatrix} \dot{\omega}_{rw}^x \\ \dot{\omega}_{rw}^y \\ \dot{\omega}_{rw}^z \end{bmatrix}, \vec{\omega}_{rw} = \begin{bmatrix} \omega_{rw}^x \\ \omega_{rw}^y \\ \omega_{rw}^z \end{bmatrix}, \vec{\omega}_{sc} = \begin{bmatrix} \omega^x \\ \omega^y \\ \omega^z \end{bmatrix}$$

and they are defined in the body axis frame. Whereas $\boldsymbol{I}_{sc}$ and $\boldsymbol{I}_{rw}$ are 3×3 matrix of moment of inertia of spacecraft and reaction wheels respectively.

d. Attitude Kinematics

Rate of change of $\boldsymbol{A}$ with respect to time is given by

$$\frac{d\boldsymbol{A}}{dt} = \begin{bmatrix} 0 & \omega^z & \omega^y \\ -\omega^z & 0 & \omega^x \\ \omega^y & -\omega^x & 0 \end{bmatrix} \boldsymbol{A} \tag{3}$$

Where $\boldsymbol{A}$ direction cosine matrix from inertial to body frame with XYZ rotation order. Orthonormalization is also performed for every integration step.

e. Orbital Kinematics

Even though we include solar radiation pressure and drag acceleration, we assume unperturbed two body problem between the spacecraft and the earth for the sake of simplicity. Therefore the only changes in Keplerian elements is true anomaly, and its changes is given by

$$\dot{\theta} = \sqrt{\frac{\mu}{a^3}} \frac{(1\dot{} + e\cos\theta)^2}{(1-e^2)^{1.5}} \tag{4}$$

f. Magnetic Torque Disturbance

The torque due to magnetic field of the earth is modeled as follows

$$\vec{b}_N = \frac{R^3 H_0}{r^3}(3(\hat{m}.\hat{r})\hat{r} - \hat{m})$$

where $\vec{b}_N$ is magnetic field vector in inertial frame,

$$H_0 = \sqrt{(g_1^0)^2 + (g_1^1)^2 + (h_1^1)^2}$$

$$\hat{m} = \begin{bmatrix} \sin 11.5^o \, cos\omega t \\ \sin 11.5^o \sin \omega t \\ \cos 11.5^o \end{bmatrix}$$

where R is earth's radius, r is spacecraft's distance from earth's center, $\hat{r}$ is unit vector of $\vec{r}$, ω is earth's angular velocity, and g_1^0, g_1^1, h_1^1 are numerical values obtained from IGRF 1995. Then magnetic field vector in body frame $\vec{b}_B$ is obtained by multiplying it with DCM $\boldsymbol{A}_{BN}$

$$\vec{b}_B = \boldsymbol{A}_{BN}.\vec{b}_B$$

Finally, parasitic magnetic torque in body frame is given by

$$\vec{M}_{mag} = \vec{m} \times \vec{b}_B \tag{5}$$

where $\vec{m}$ is residual magnetic induction due to parasitic currents in the spacecraft.

g. Gravity Gradient Torque

Gravity gradient torque is modeled as follows

$$\vec{M}_{gg} = \frac{3\mu}{R^3} \begin{bmatrix} (I_z - I_y)c_2c_3 \\ (I_x - I_z)c_1c_3 \\ (I_y - I_x)c_1c_2 \end{bmatrix} \tag{6}$$

where $\vec{c} = [c_1 \quad c_2 \quad c_3]^\top$ is direction from earth's center to spacecraft in body frame axis.

h. Solar Radiation Pressure

Torque due to solar radiation pressure is modeled as follows

$$\vec{F}_i = -PA_i(\hat{S}_B.\hat{N}_{Bi})\left[(1-\rho_s)\hat{S}_B + \left(2\rho_s(\hat{S}_B.\hat{N}_{Bi}) + \frac{2}{3}\rho_d\right)\hat{N}_{Bi}\right] \tag{7}$$

where $\vec{F}_i$ is solar radiation force acting on surface i in body frame, $\hat{S}_B$ is spacecraft to sun direction in body frame, $\hat{N}_{Bi}$ is normal direction of surface i in body frame, and P is defined as

$$P = \frac{F_e}{C}, F = 1358\, W/m^2, C = 299792458\, m/s$$

Therefore, the torque due to solar radiation pressure $\vec{T}_{SRP}$ can be written as

$$\vec{T}_{SRP} = \begin{cases} \sum_{i=1}^{n} \vec{r}_i \times \vec{F}_i \ \ for\ \hat{S}_B.\hat{N}_{Bi} > 0 \\ 0\ for\ \hat{S}_B.\hat{N}_{Bi} \ \leq 0 \end{cases} \quad (8)$$

i. Attitude Sensors

Three sensors are used to compute the attitude of spacecraft, they are sun sensor, earth sensor, and star sensor, but they are modeled in a simple way. It is assumed that the objects are always visible with respect to the sensor, therefore the output of the sensor is a vector direction of the object in the body frame axis. For star sensor, it is assumed that the star sensor is always able to see one fixed star and therefore the output is star's direction vector in body axis frame.

j. Gyroscope

Gyroscope is used to measure the angular velocity of spacecraft in body frame and is modeled as follows

$$\vec{\omega} = \vec{\omega}^{real} + \vec{n} + \vec{b} \quad (9)$$

where $\vec{n}$ and $\vec{b}$ are zero mean white noise

$$\vec{n} = \sigma_n \vec{\eta}_n, \dot{\vec{b}} = \sigma_b \vec{\eta}_b$$

and

$$\sigma_n = \frac{ARW}{\sqrt{T_s}}, \sigma_b = \frac{RRW}{\sqrt{T_s}}$$

Then the dynamics of gyroscope is modeled as

$$\begin{aligned} \ddot{\theta}_x &= -\frac{1}{J_z}\left[c\ \dot{\theta}_x + k\ \theta_x + I_r \omega_r \omega_x\right] \\ \ddot{\theta}_y &= -\frac{1}{J_z}\left[c\ \dot{\theta}_y + k\ \theta_y + I_r \omega_r \omega_y\right] \\ \ddot{\theta}_z &= -\frac{1}{J_z}\left[c\ \dot{\theta}_z + k\ \theta_z + I_r \omega_r \omega_z\right] \end{aligned} \quad (10)$$

By solving numerically equation (10) we can obtain θ_x, θ_y, and θ_z. Finally, the measured angular velocity is computed by

$$\begin{aligned} \omega_x^{raw} &= -\frac{k\ \theta_x}{I_r \omega_r} \\ \omega_y^{raw} &= -\frac{k\ \theta_y}{I_r \omega_r} \\ \omega_z^{raw} &= -\frac{k\ \theta_z}{I_r \omega_r} \end{aligned} \quad (11)$$

This raw measured angular velocity still needs to be filtered because it contains noises.

k. Attitude Determination

SVD method is used to solve the DCM between vectors from the sensors and from inertial reference frame

$$\boldsymbol{A} = \boldsymbol{U}\boldsymbol{M}\boldsymbol{V}^{\top}$$

where $\boldsymbol{U}$, $\boldsymbol{M}$, and $\boldsymbol{V}$ are obtained from

$$\boldsymbol{U}\boldsymbol{S}\boldsymbol{V}^{\top} = svd(\boldsymbol{B})$$

$$\boldsymbol{M} = diag[1\ 1\ \det(\boldsymbol{U})\,.\det(\boldsymbol{V})] \tag{10}$$

where

$$\boldsymbol{B} = \sum_{\boldsymbol{i}}^{\boldsymbol{n}} \alpha_{\boldsymbol{i}} \vec{s}_{Bi} \vec{u}_{Ni}^{T}$$

where $\alpha_{\boldsymbol{i}}$ is the weight for each measurement vector and is defined

$$\sum_{\boldsymbol{i}}^{\boldsymbol{n}} \alpha_{\boldsymbol{i}} = 1$$

l. Filtering

We used a state observer since making use of a frequency-based low pass filter would be unsuitable for real time processing because it would result in an excessive phase delay which means a delay control input. A state observer is given by

$$\dot{\hat{\boldsymbol{x}}} = f(\hat{\boldsymbol{x}}, \boldsymbol{u}) + G(\hat{\boldsymbol{y}} - \boldsymbol{y}) \tag{11}$$

where $\hat{\boldsymbol{x}}$ is the estimated state, $f(\hat{\boldsymbol{x}}, \boldsymbol{u})$ is the equation governing $\dot{\hat{\boldsymbol{x}}}$ as a function of $\hat{\boldsymbol{x}}$ and control input $\boldsymbol{u}$, G is a gain, $\hat{\boldsymbol{y}}$ is estimated output, and $\boldsymbol{y}$ is unfiltered output coming from sensor.

m. Control Algorithm

For de-tumbling, a simple feedback proportional control algorithm is used which given by

$$\boldsymbol{u} = -k\vec{\omega}_{sc} \tag{12}$$

where $\boldsymbol{u}$ is control torque and k is gain. While for nadir pointing, we used DCM-based control law which is given by

$$\boldsymbol{u} = -k_1\vec{\omega}_e - k_2[\boldsymbol{A}_{\boldsymbol{e}}^{\top} - \boldsymbol{A}_{\boldsymbol{e}}]^{V} + \vec{\omega}_{sc} \times \boldsymbol{J}\vec{\omega}_{sc} + \boldsymbol{J}(\boldsymbol{A}_{\boldsymbol{e}}\dot{\vec{\omega}}_d - \vec{\omega}_e \times \boldsymbol{A}_{\boldsymbol{e}}\vec{\omega}_d) \tag{13}$$

where $\boldsymbol{J}$ is total mass of inertia, $\boldsymbol{A_e} = \boldsymbol{A}\boldsymbol{A_d^T}$, $\vec{\omega}_e = \vec{\omega}_{sc} - \boldsymbol{A_e}\vec{\omega}_d$, $\boldsymbol{A_d}$ is desired DCM, and $\vec{\omega}_d$ is desired angular velocity. For nadir pointing, $\boldsymbol{A_d}$ is defined as

$$\boldsymbol{A_d} = \begin{bmatrix} \cos(\theta+\omega) & \sin(\theta+\omega) & 0 \\ -\sin(\theta+\omega) & \cos(\theta+\omega) & 0 \\ 0 & 0 & 1 \end{bmatrix} \begin{bmatrix} 1 & 0 & 0 \\ 0 & \cos i & \sin i \\ 0 & -\sin i & \cos i \end{bmatrix} \begin{bmatrix} \cos\Omega & \sin\Omega & 0 \\ -\sin\Omega & \cos\Omega & 0 \\ 0 & 0 & 1 \end{bmatrix}$$

and $\vec{\omega}_d$ is

$$\vec{\omega}_d = [0 \quad 0 \quad \dot{\theta}]^{\mathsf{T}}$$

Once $\boldsymbol{u}$ is computed, we can compute $\vec{\omega}_{rw}$ and $\dot{\vec{\omega}}_{rw}$ using equation (2).

III. Data for Simulation

The following data are used during simulation

Table 2. Initial Keplerian elements.

a	e	i	Ω	ω	θ
7500 km	0.1	10°	40°	60°	0°

Table 3. Gyroscope STIM202 by Sensonor.

ARW	RRW	Sampling rate
0.2 deg/h$^{0.5}$	0.3 deg/h	1000 Hz

Table 4. Sun sensor SS200 by Hyperion Technologies, B.V.

Accuracy	FoV	Sampling rate
< 1°	110°	100 Hz

Table 5. Earth Horizon Sensor MAI-SES by Maryland Aerospace, Inc.

Accuracy	FoV	Sampling rate
< 0.25°	7°	100 Hz

Table 6. Sagitta Star Tracker by Arcsec.

Accuracy	Lost-in-space availability	Sampling rate
< 10 arc seconds	99%	10 Hz

Table 7. Reaction wheel RW400 by Hyperion Technologies.

Mass	Dimensions	Maximum speed	Maximum torque
340 g	50×50×27 mm	6000 RPM (628.3 rad/s)	12 mN.m

IV. Results and Discussions

Here we present the results of simulation for various cases: de-tumbling for 50 seconds, nadir pointing for 100 seconds, and nadir pointing for 1 full orbit.

a. De-tumbling

We simulated de-tumbling for 50 seconds using initial DCM $\boldsymbol{A} = \boldsymbol{I}$ and initial angular velocity of spacecraft $\boldsymbol{\omega} = [5\ 10\ -7]^{\mathrm{T}}\ deg/s$. We used 2 different value of k for de-tumbling control law, that is k = 0.5 and k = 0.05, and the results are given as follows

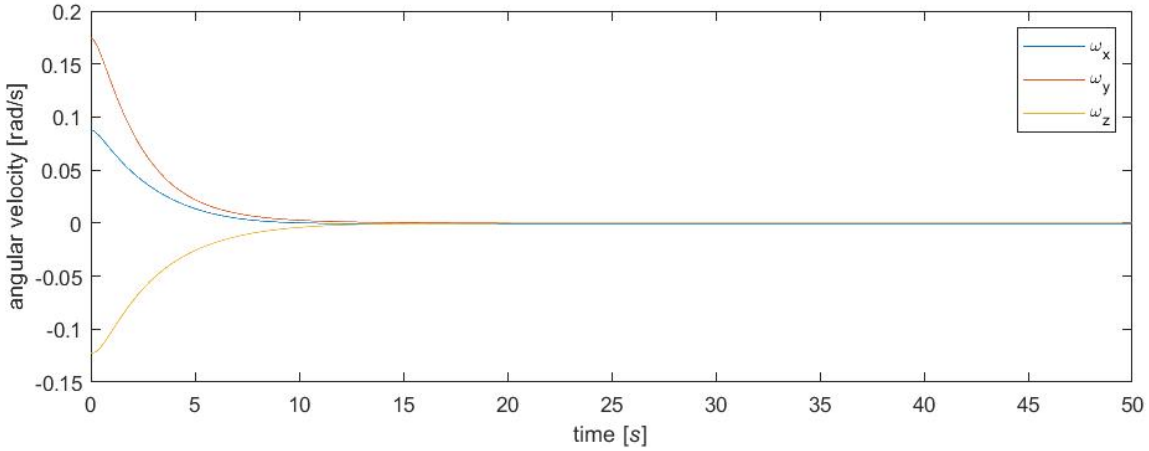

Figure 3. Angular velocity of spacecraft using k = 0.5.

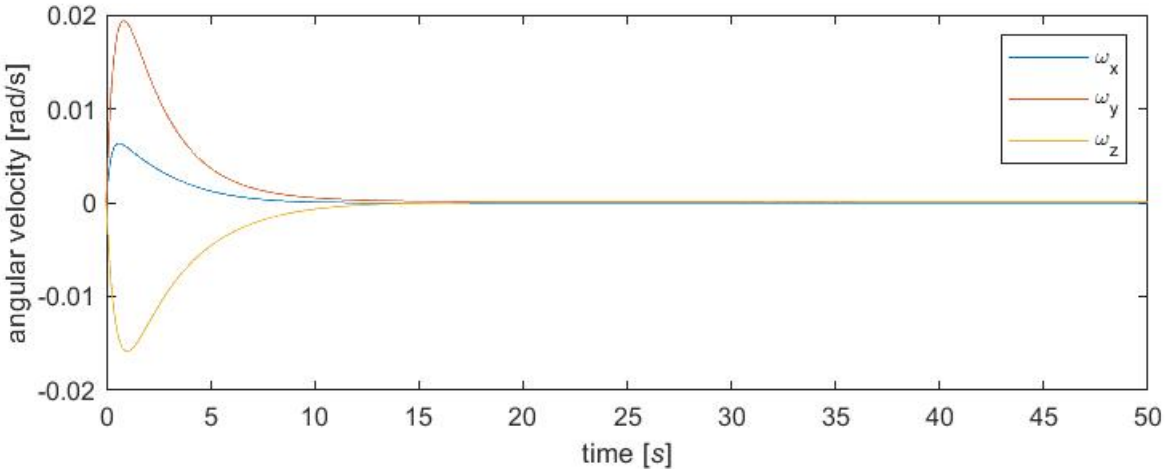

Figure 4. Estimated angular velocity of spacecraft from state observer using k = 0.5.

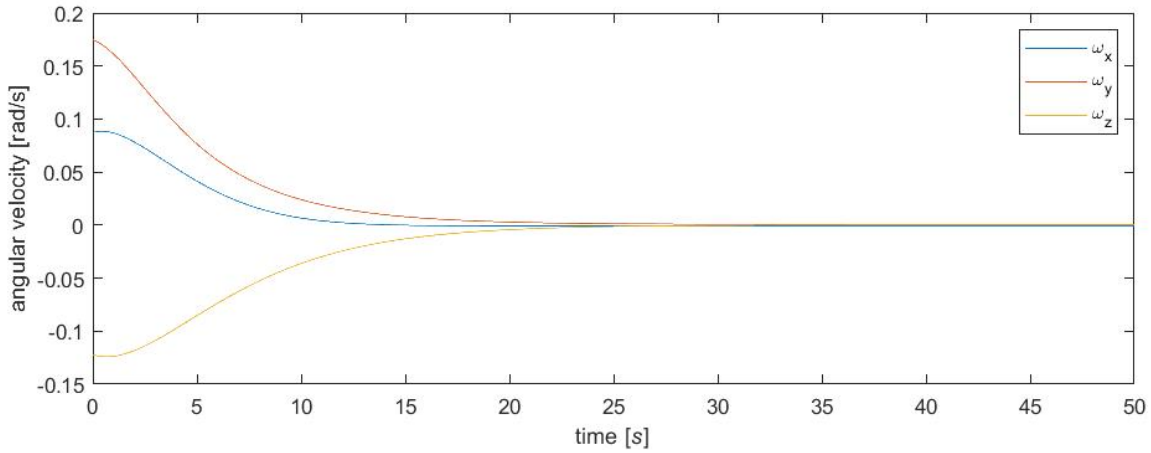

Figure 5. Angular velocity of spacecraft using k = 0.05

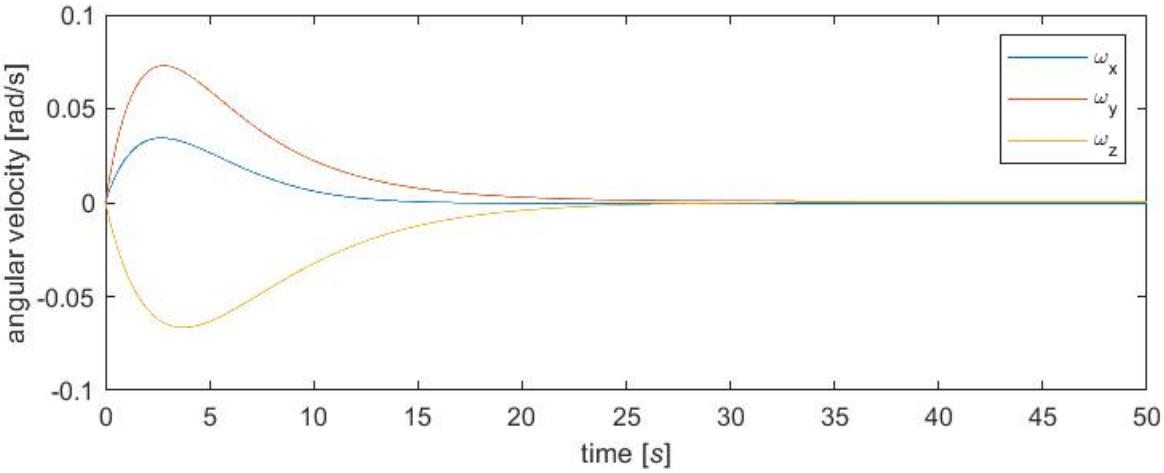

Figure 6. Estimated angular velocity of spacecraft from state observer using k = 0.05.

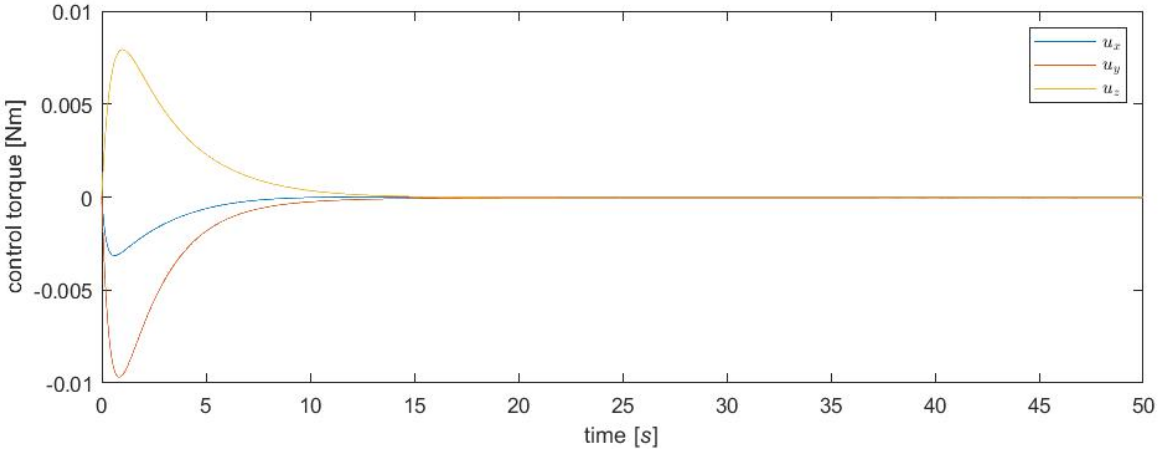

Figure 7. Control torque for de-tumbling using k = 0.5.

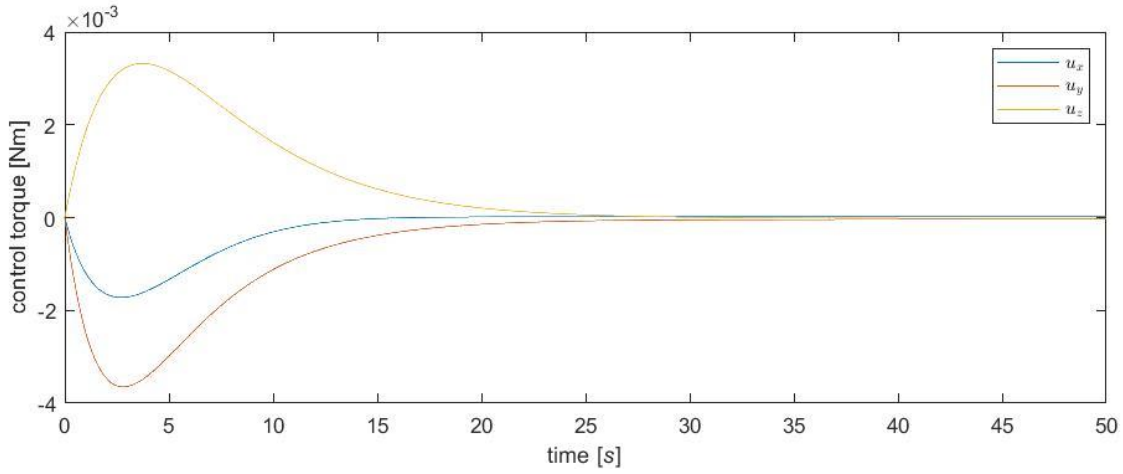

Figure 8. Control torque for de-tumbling using k = 0.05.

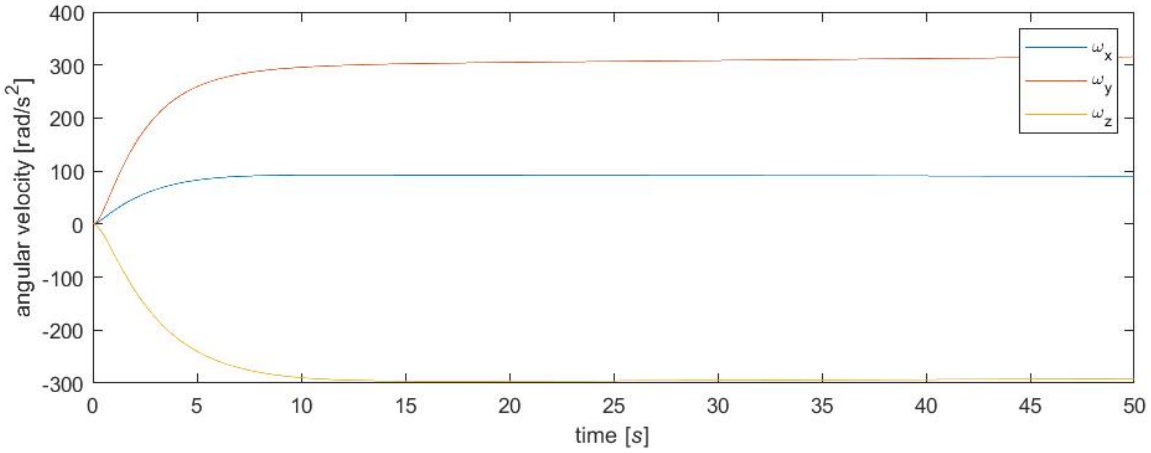

Figure 9. Angular velocity of reaction wheels using k = 0.5.

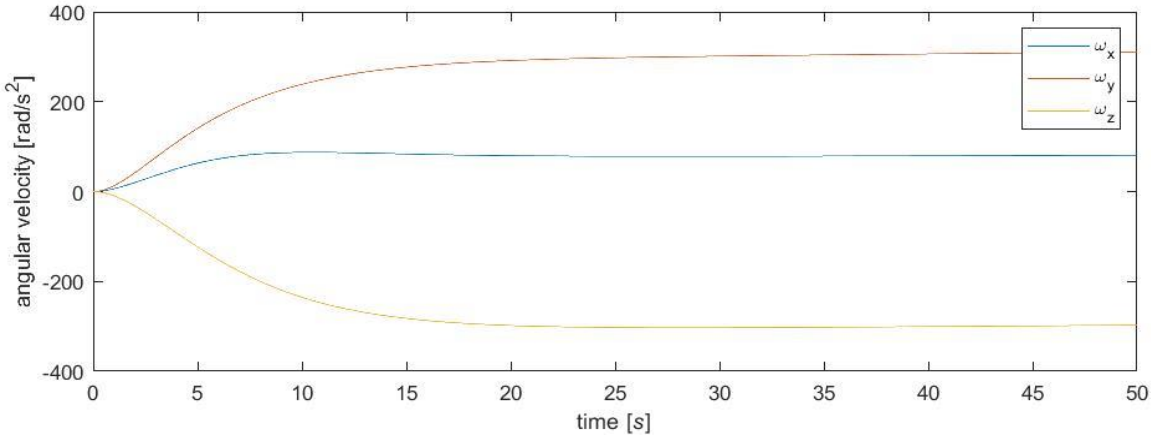

Figure 10. Angular velocity of reaction wheels using k = 0.05.

From the results above it is obvious that the larger k the faster for spacecraft to achieve de-tumbling, but it costs more control torque. Note that from figure 3 for k = 0.5 the spacecraft is brought to rest within 15 seconds but 8 mN.m of control torque is required.

While for k = 0.05 the spacecraft achieves zero angular velocity within 30 seconds, and the required control torque is only 3.5 mN.m at its peak. It clearly shows that there is a tradeoff in tuning the value of k. Nevertheless, for both value of k, the rotation speed of reaction wheels is still below the maximum value which is 628.3 rad/s.

b. Nadir Pointing

Here we simulated nadir pointing for 100 seconds using initial DCM $\boldsymbol{A} = \boldsymbol{I}$ and initial angular velocity of spacecraft $\boldsymbol{\omega} = [5\ 10\ -7]^{\mathrm{T}}\ deg/s$. We used k_1 = 0.25 and k_2 = 0.01 for control law.

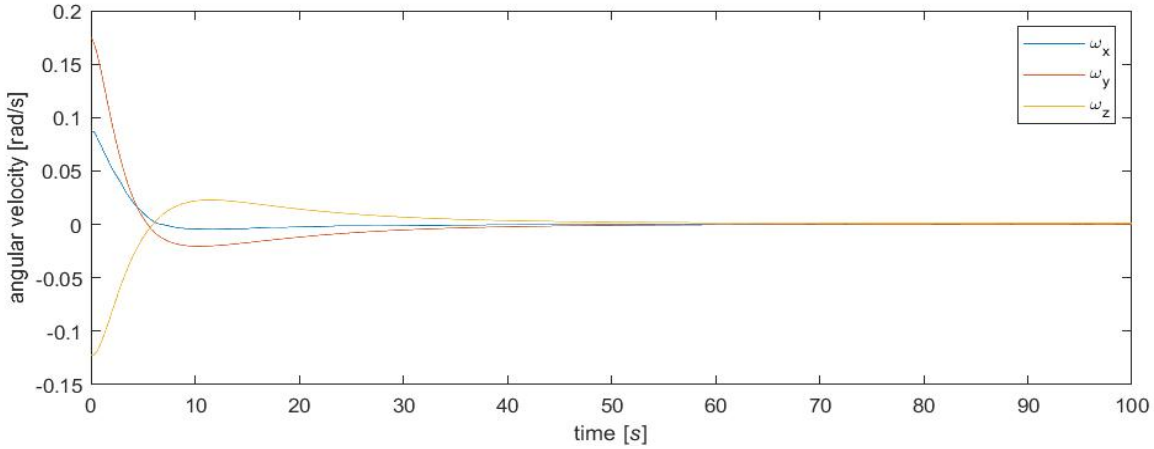

Figure 11. Angular velocity of spacecraft during nadir pointing.

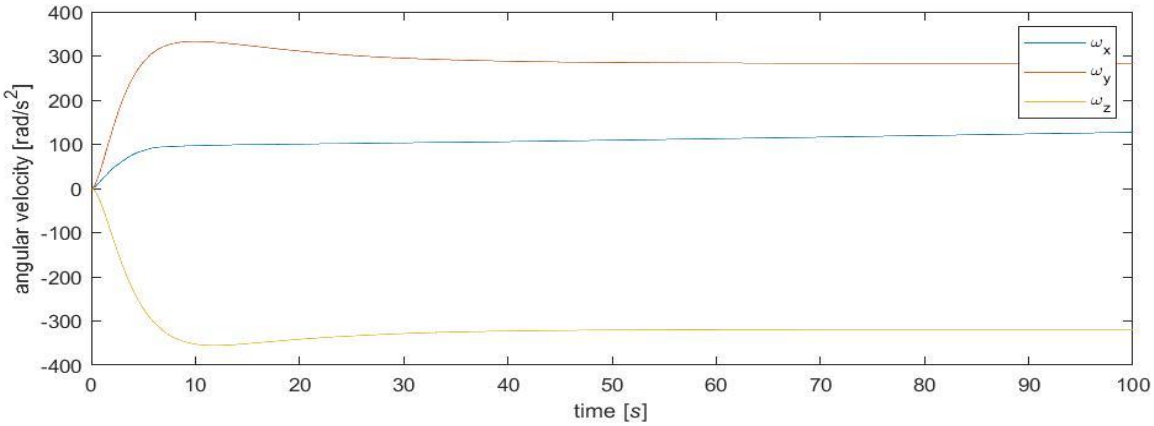

Figure 12. Angular velocity of reaction wheels for nadir pointing.

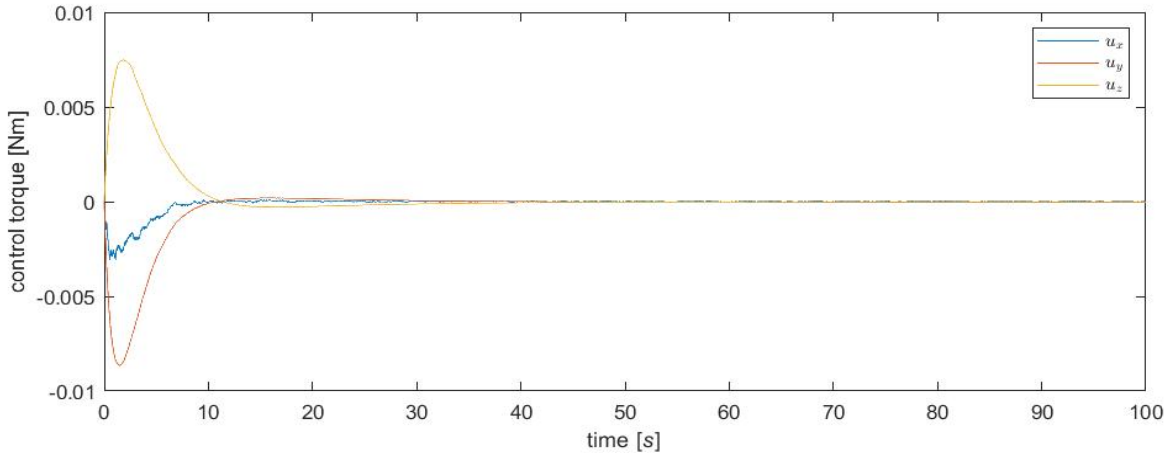

Figure 13. Control torque for nadir pointing.

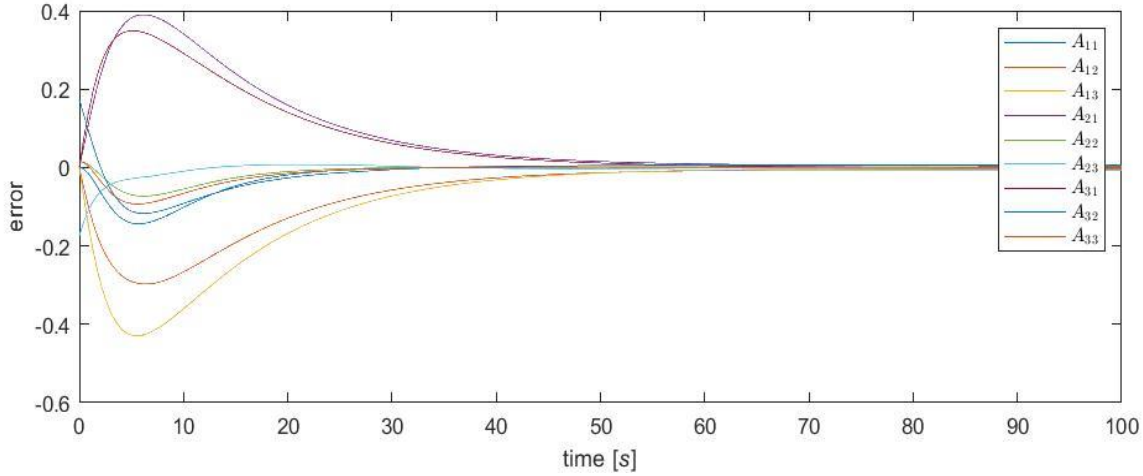

Figure 14. Error components of DCM matrix.

For nadir pointing we can inspect from figure 14 that the manoeuvre is successfully performed within 70 seconds from initial attitude. Moreover, angular velocity of reaction wheels are still within its maximum limit, but we have to check for one full revolution orbit if there is any saturation. And also, from figure 13 we can see that the maximum torque required is only around 8 mN.m which is still below maximum value.

c. Nadir Pointing for 1 Full Orbit

Here we simulated nadir pointing for 1 full orbit.

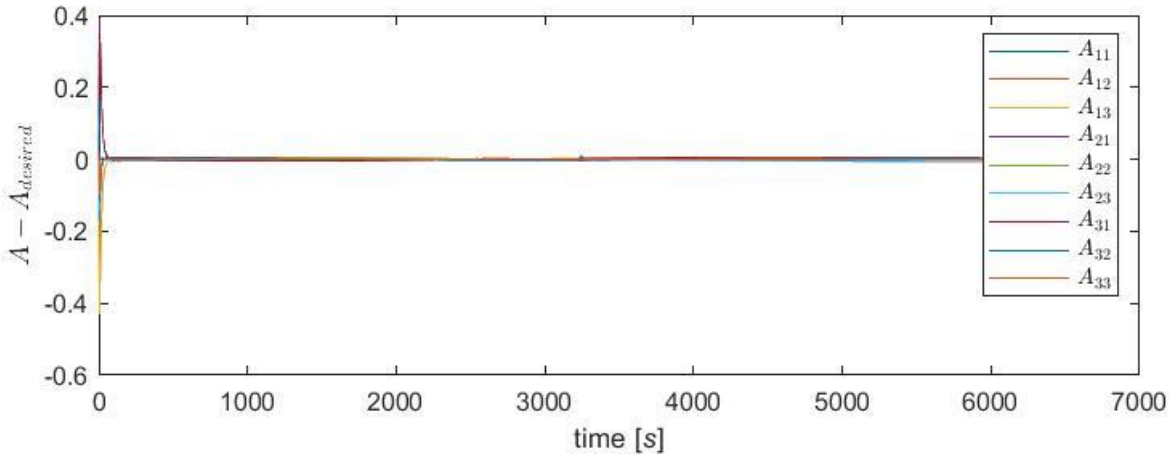

Figure 15. DCM error.

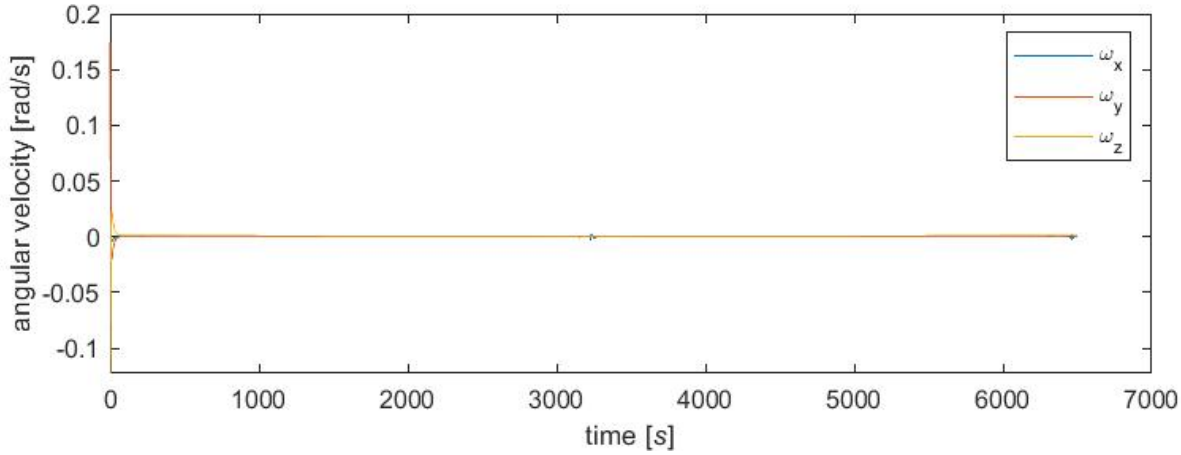

Figure 16. Angular velocity of spacecraft for 1 full orbit.

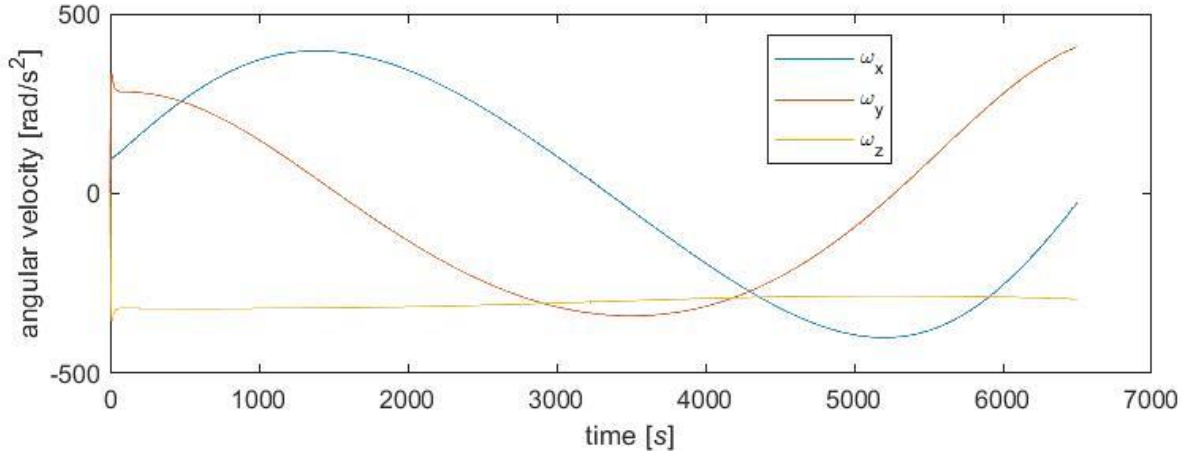

Figure 17. Angular velocity of reaction wheels for 1 full orbit.

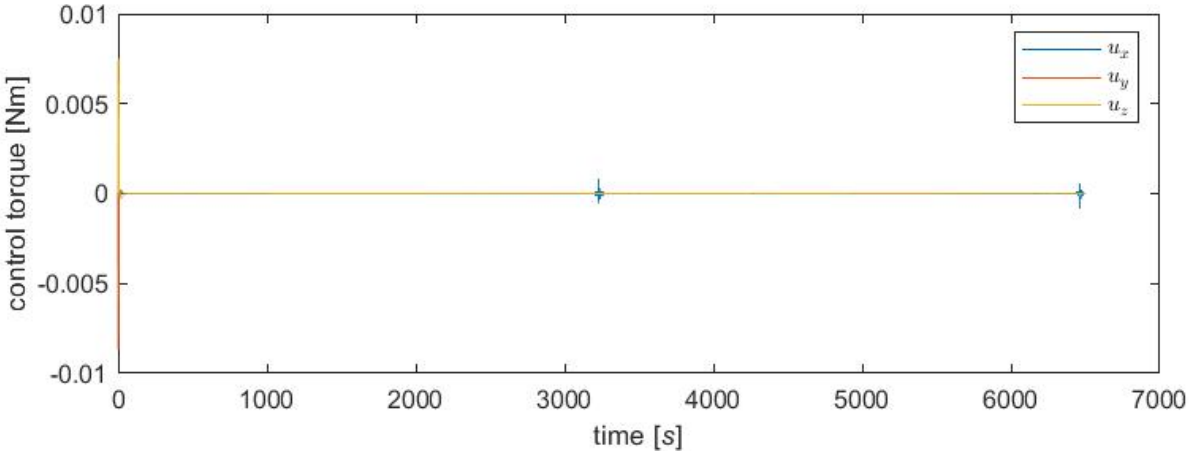

Figure 18. Control torque required for nadir pointing during 1 full orbit.

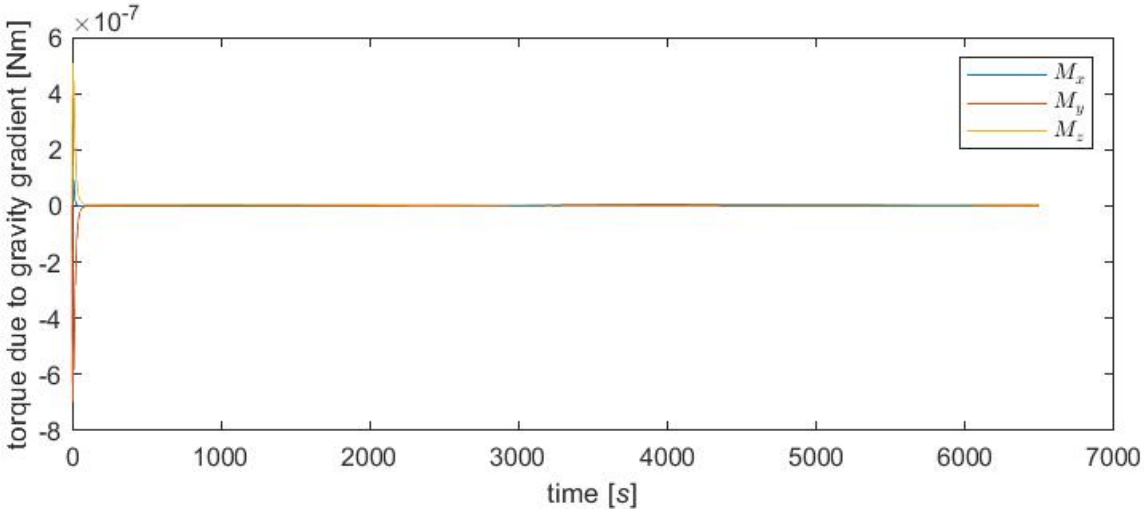

Figure 19. Gravity gradient torque for 1 full orbit.

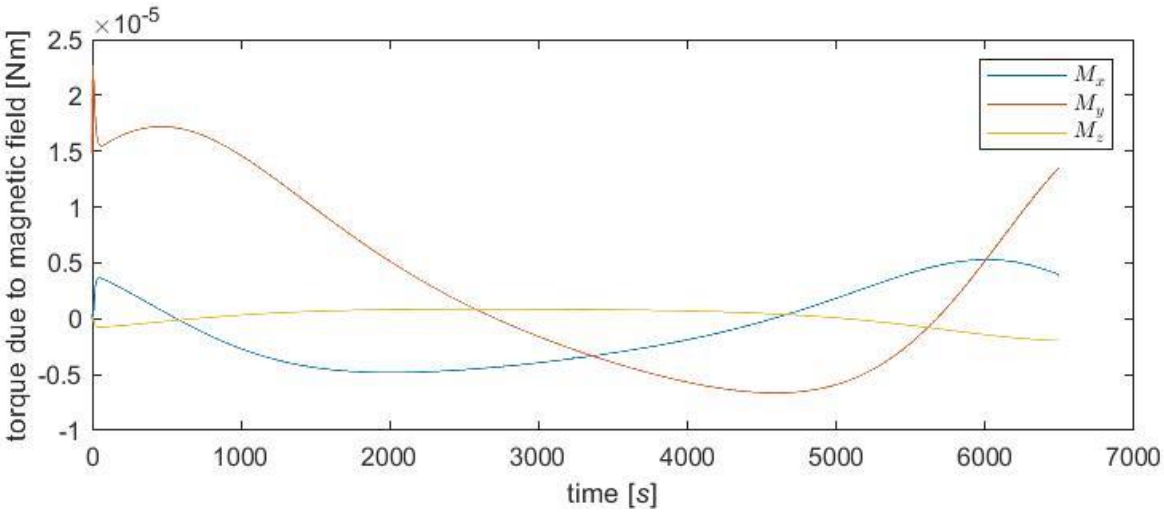

Figure 20. Disturbance torque due to magnetic field for 1 full orbit.

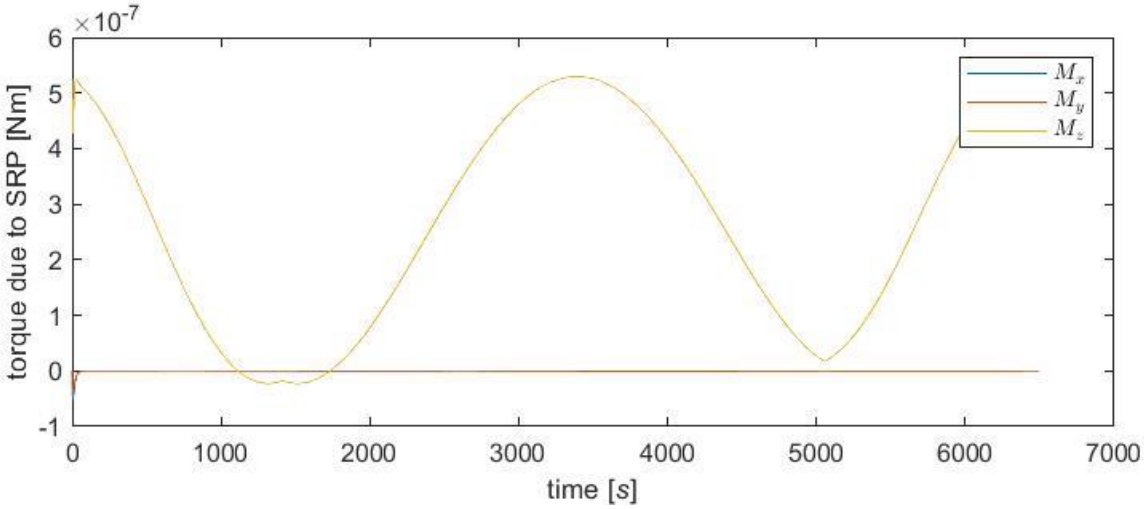

Figure 21. Disturbance torque due to SRP for 1 full orbit.

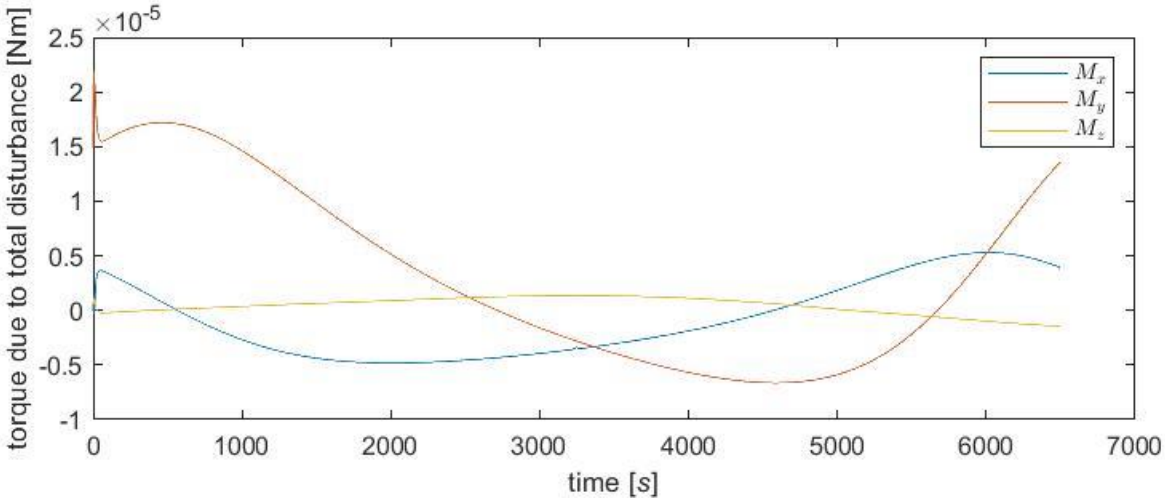

Figure 22. Total disturbance torque during 1 full orbit.

From figure 17 we can clearly see that the angular velocities of reaction wheels are still below maximum value provided by RW400, therefore we do not need to provide any redundant actuators. Moreover, from figure 18 we see that the control torque required is very small, and its peak is only at the beginning. This is due to the fact that nadir pointing only requires a very small angular velocity around z axis of body frame. While from figure 18 we can see that after desired DCM for nadir pointing is achieved, the gravity gradient torque acting on the spacecraft is very small, and this is because when in nadir pointing position, spacecraft is in symmetric attitude with respect to earth direction, therefore the net torque due to gravity gradient is almost negligible. While for magnetic field and SRP disturbance torque, the value is periodic. From those three disturbance torques, we can say that the most prominent one is magnetic field torque.

V. Conclusions

From the results and discussions, we can conclude that both de-tumbling and nadir pointing are successfully achieved. De-tumbling is performed within reasonable time and needs only small control torque which still below maximum value provided by RW400. The reaction wheels also didn't saturate during this manoeuvre. We can still further exploit other possible value of k for de-tumbling control law, or even implement other control logic such as LQR. Nadir pointing was also achieved within reasonable time. And also according to the results of full one orbit simulation, we can also conclude that we do not need any redundant actuators since all three reaction wheels did not saturate during this period.

VI. References

(n.d.). Retrieved from https://www.sensonor.com/products/gyro-modules/stim202/

(n.d.). Retrieved from https://hyperiontechnologies.nl/products/ss200/

(n.d.). Retrieved from https://www.cubesatshop.com/wp-content/uploads/2016/06/MAI-SES-Specifications-20150827.pdf

(n.d.). Retrieved from https://www.cubesatshop.com/product/kul-star-tracker/#:~:text=The%20Sagitta%20star%20tracker%20offers,the%20effect%20of%20stray%20light.

(n.d.). Retrieved from https://hyperiontechnologies.nl/products/rw400-series-reaction-wheel/

Markley, F. L. (2014). *Fundamentals of Spacecraft Attitude Determination and Control.* London: Springer.

Zazzera, F. B. (n.d.). *Course Notes Spacecraft Attitude Dynamics and Control Part 1: Attitude Dynamics and Kinematics.*

Zazzera, F. B. (n.d.). *Course Notes Spacecraft Attitude Dynamics and Control Part 2: Attitude Determination and Control Systems.*